Interaction Notes

Note 131

October 1972

(revised April 1974)

L-SHAPED WIRE OVER A GROUND PLANE

By

Clayborne D. Taylor
Physics Department
Mississippi State University
Mississippi State, Mississippi

L-shaped wires, ground plane, conduction

ABSTRACT

An L-shaped wire illuminated by a plane wave is considered oriented over a ground plane with one segment parallel to the ground plane and the other perpendicular. An integral equation is derived for the current distribution and is solved by the method of moments. Some numerical data are presented for an L-shaped wire representing an aircraft. Both frequency domain and time domain data are included.

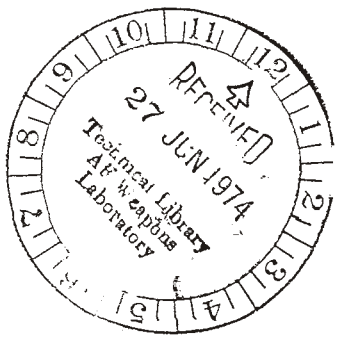

INTRODUCTION

The current distribution induced on an L-shaped wire is obtained for the wire being illuminated by a plane wave propagating normally to the plane of the wire. First the L-shaped wire is considered to be in free space (see Figure 1) and second the wire is considered to be oriented over a perfectly conducting ground plane so that one leg of the L is parallel to the ground plane and the other perpendicular (see Figure 2). An integral equation for the current distribution is obtained for the induced current distribution by considering the wire formed by two intersecting wires and requiring the continuity of current and potential be imposed at the junction.[1] To account for the presence of the ground plane images are used.

A numerical solution for the integral equation is obtained by employing the method of moments. In the solution technique the current distribution is represented by a finite sum of square pulses. This particular expansion is used because it obviates the need for double integration that would occur for other commonly used expansions. Further the pulses are constrained so that every other pulse height is the average of the adjacent pulse heights. This yields a rapidly convergent solution, yet it is efficient in so far as computation time is concerned. The current distribution is obtained for harmonic time dependence first and then Fourier frequency superposition is employed for the case of a transient incident field.

Some numerical data are presented for an L-shaped wire representing an aircraft. And a few general observations are proffered. A parametric

study is not presented but one is in preparation where Baum's singularity expansion technique is being used.[5]

ANALYSIS

L-Shaped Wire in Free Space

The integral equation for the current distribution induced on a system of N wires is[1]

$$\sum_{m=1}^{N} \int_{L_m} ds'_m \, I_m(s'_m) \, \Pi(s_n,s'_m) = C_n \cos ks_n + D_n \sin ks_n - j \frac{4\pi}{\zeta} \int_0^{s_n} ds'_n \, E^{inc}_{s_n}(s'_n) \sin k(s_n - s'_n) \tag{1}$$

where

$$\Pi(s_n,s'_m) = G(s_n,s'_n)(\hat{s}'_m \, \hat{s}_n) - \int_0^{s_n} ds'_n \cos k(s_n - s'_n) \left[\frac{\partial}{\partial s'_m} G(s'_n,s'_m) + \frac{\partial}{\partial s'_n} [G(s'_n,s'_m)(\hat{s}'_m \cdot \hat{s}'_n)] \right] \tag{2}$$

$$G(s_n,s'_m) = \exp \left[-jk \sqrt{r^2(s_n,s'_m) + a_m^2} \right] / \sqrt{r^2(s_n,s'_m) + a_m^2} \tag{3}$$

with $r(s_n,s'_m)$ as the linear distance between point s_n on the nth wire and the point s'_m on the mth wire, a_m the radius of the mth wire, L_m the length of the mth wire, $\hat{s}_m$ the unit vector parallel to the axis of the mth wire at point s_m, and $E^{inc}_{s_m}(s_m)$ the component of the electric field parallel to the axis of the mth wire at point s_m.

If a single L-shaped wire is considered it must be considered as two wires, one horizontal and one vertical. Applying (1) - (3) to this wire configuration yields the following integral equations (see Figure 1) for $-\ell_f \leq s_1 \leq 0$

$$\int_{-\ell_f}^{0} ds'_1 \, I_1(s'_1) K_{11}(s_1,s'_1) - \int_0^{\ell_t} ds'_2 \, I_2(s'_2) \frac{\partial}{\partial s'_2} K_{12}(s_1,s'_2) = C_1 \cos ks_1 + D_1 \sin ks_1 - j \frac{4\pi}{\zeta} \int_0^{s_1} ds'_1 \, E^{inc}_{s_1}(s'_1) \sin k(s_1 - s'_1) \tag{4}$$

and for $0 \leq s_2 \leq \ell_t$

$$- \int_{\ell_f}^{0} ds_1' \, I_1(s_1') \frac{\partial}{\partial s_1'} K_{21}(s_2,s_1') + \int_{0}^{\ell_t} ds_2' \, I_2(s_2') K_{22}(s_2,s_2')$$

$$= C_2 \cos ks_2 + D_2 \sin ks_2 - j \frac{4\pi}{\zeta} \int_{0}^{s_2} ds_2' \, E^{inc}_{s_2}(s_2') \sin k(s_2 - s_2') \tag{5}$$

where

$$K_{11}(s_1,s_1') = \exp\left[-jk\sqrt{(s_1 - s_1')^2 + a_f^2} \right] \Big/ \sqrt{(s_1 - s_1')^2 + a_f^2} \tag{6}$$

$$K_{12}(s_1,s_2') = \int_{0}^{s_1} ds_1' \cos k(s_1 - s_1') \frac{e^{-jk\sqrt{s_1'^2 + s_2'^2 + a_f^2}}}{\sqrt{s_1'^2 + s_2'^2 + a_f^2}} \tag{7}$$

$$K_{21}(s_2,s_1') = \int_{0}^{s_2} ds_2' \cos k(s_2 - s_2') \frac{e^{-jk\sqrt{s_2'^2 + s_1'^2 + a_t^2}}}{\sqrt{s_2'^2 + s_1'^2 + a_t^2}} \tag{8}$$

$$K_{22}(s_2,s_2') = \exp\left[-jk\sqrt{(s_2 - s_2')^2 + a_t^2} \right] \Big/ \sqrt{(s_2 - s_2')^2 + a_t^2} \tag{9}$$

By requiring wire #1 at $s_1 = 0$ to be at the same potential as wire #2 at $s_2 = 0$, the following is obtained:

$$D_1 = D_2 \tag{10}$$

In order to obtain a unique solution for the current distribution the following boundary conditions on the current must be applied:

$$I_1(-\ell_f) = 0$$

$$I_2(\ell_t) = 0$$

$$I_1(0) = I_2(0)$$

The foregoing integral equations may be solved conveniently by using standard numerical solution techniques. Perhaps the most convenient employs the so called pulse expansion for the unknown current distribution and point matching.[2] That is, the current is represented

$$I_1(s_1') = \sum_{n=1}^{N} f_n[H(s_1' - s_{1n}')H(s_{1,n+1}' - s_1')] \tag{14}$$

$$I_2(s_2') = \sum_{n=1}^{M} g_n(H(s_2' - s_{2n}')H(s_{2,n+1}' - s_2')] \tag{15}$$

where

$$H(x) = 0 \qquad x < 0$$

$$= 1 \qquad x > 0$$

and $\{s_{1n}'\}$ and $\{s_{2n}'\}$ are ordered sets of points on the range $-\ell_f \leq s_1 \leq 0$ and $0 \leq s_2 \leq \ell_t$ respectively (see Figure 1).

Substituting (14) and (15) into (4) and (5) and satisfying the integral equations at a suitable discrete set of points yields a system of linear complex equations, such as

$$\sum_{n=1}^{N+M} \Pi_{mn} F_n = \Gamma_m \tag{16}$$

where for m = 1, N

$$\Pi_{m1} = -\cos ks_{1m}$$

$$\left.\begin{aligned} \Pi_{mn} &= \int_{s_{1n}'}^{s_{1,n+1}'} ds_1' \, K_{11}(s_{1m}, s_1') \qquad n = 2, 3, \cdots N-1 \\ \Pi_{mN} &= \int_{-\Delta/2}^{0} ds_1'[K_{11}(s_{1m} \cdot s_1')] - K_{12}(s_{1m}, \Delta/2) + K_{12}(s_{1m}, 0) \end{aligned}\right\}$$

$$\Pi_{m,N-1+n} = -K_{12}(s_{1m},s'_{2,n+1}) + K_{12}(s_{1m},s'_{2n}) \qquad n=2,3,\cdots M-1$$

$$\Pi_{m,N+M-1} = 0 \ .$$

$$\Pi_{m,N+M} = -\sin ks_{1m}$$

$$\Gamma_m = -j\frac{4\pi}{\zeta}\int_0^{s_{1m}} ds'_1\, E^{inc}_{s_1}(s'_1)\sin k(s_{1m}-s'_1) \qquad (17)$$

for $m=N+1,N+M$

$$\Pi_{m1} = 0 \ .$$

$$\Pi_{mn} = -K_{21}(s_{2,m-N},s'_{1,n+1}) + K_{21}(s_{2,m-N},s'_{1n}) \qquad n = 2,3,\cdots N-1$$

$$\Pi_{mN} = -K_{21}(s_{2,m-N},0) + K_{21}(s_{2,m-N},-\Delta/2) + \int_0^{\Delta/2} ds'_2\, K_{22}(s_{2,m-N},s'_2)$$

$$\Pi_{m,N-1+n} = \int_{s'_{2n}}^{s'_{2,n+1}} ds'_2\, K_{22}(s_{2,m-N},s'_2) \qquad n = 2,3,\cdots M-1 \qquad (18)$$

$$\Gamma_m = -j\frac{4\pi}{\zeta}\int_0^{s_{2,m-N}} ds'_2\, E^{inc}_{s_2}(s'_2)\sin k(s_{2,m-N}-s'_2)$$

$$\Pi_{m,N+M-1} = \cos(ks_{2,m-N})$$

$$\Pi_{m,N+M} = -\sin(ks_{2,m-N})$$

with

$$s'_{1n} = -\ell_f + (n-3/2)\Delta$$

$$s_{1n} = \ell_f + (n-1)\Delta \tag{19}$$

$$s'_{2n} = (n-3/2)\Delta$$

$$s_{2n} = (n-1)\Delta$$

$$F_n = \begin{cases} f_n & n=1,N \\ g_{n-N} & n=N+1,N+M \end{cases}$$

and

$$\Delta = \frac{\ell_f}{N-1} = \frac{\ell_t}{M-1} \tag{20}$$

defining the point sets that may be used.

L-Shaped Wire Over a Ground Plane

When the L-shaped wire is located over a ground plane the effect of the ground may be incorporated by use of images(see Figure 2). The image of the L-shaped wire carries an equal but oppositely directed current on each segment as on the corresponding segment of the L-shaped wire. Although (1) still applies the problem now has four wires, but pairs of the wires have related current distributions. Using this information in (1) yields the following coupled integral equations:

for $-\ell_f \le s_1 \le 0$

$$\int_{-\ell_f}^{0} ds'_1\, I_1(s'_1) K^d_{11}(s_1,s'_1) - \int_{0}^{\ell_t} ds'_2\, I_2(s'_2) \frac{\partial}{\partial s'_2} K^d_{12}(s_1,s'_2)$$

$$= C_1 \cos ks_1 + D_1 \sin ks_1 - j\frac{4\pi}{\zeta} \int^{s_1} ds'_1\, E^d_{s_1}(s'_1) \sin k(s_1 - s'_1) \tag{21}$$

and for $0 \leq s \leq \ell_t$

$$-\int_{-\ell_f}^{0} ds_1' \, I_1(s_1') \frac{\partial}{\partial s'} K_{21}^d(s_2,s_1') + \int_0^{\ell_t} ds_2' \, I_2(s_2') K_{22}^d(s_2,s_2')$$

$$= C_2 \cos ks_2 + D_2 \sin ks_2 - j\frac{4\pi}{\zeta}\int_0^{s_2} ds_2' E_{s_2}^d(s_2') \sin k(s_2 - s_2') \qquad (22)$$

where

$$K_{11}^d(s_1,s_1') = K_{11}(s_1,s_1') - \frac{e^{-jk\sqrt{(s_1 - s_1')^2 + 4d^2}}}{\sqrt{(s_1 - s_1')^2 + 4d^2}}$$

$$K_{12}^d(s_1,s_2') = K_{12}(s_1,s_2') + \int_0^{s_1} ds_1' \cos k(s_1 - s_1') \frac{e^{-jk\sqrt{s_1'^2 + (2d + s_2')^2}}}{\sqrt{s_1'^2 + (2d + s_2')^2}}$$

$$K_{22}^d(s_2,s_2') = K_{22}(s_2,s_2') + \frac{e^{-jk\sqrt{(s_2 + s_2' + 2d)^2 + a_t^2}}}{\sqrt{(s_2 + s_2' + 2d)^2 + a_t^2}}$$

$$K_{21}^d(s_2,s_1') = K_{21}(s_2,s_1') - \int_0^{s_2} ds_2' \cos k(s_2 - s_2') \frac{e^{-jk\sqrt{s_1'^2 + (2d + s_2')^2}}}{\sqrt{s_1'^2 + (2d + s_2')^2}}$$

and

$$E_{s_1}^d(s_1') = E_{s_1}^{inc}(s_1') + E_{s_1}^{ref}(s_1')$$

$$E_{s_2}^d(s_2') = E_{s_2}^{inc}(s_2') + E_{s_2}^{ref}(s_2')$$

with E_s^{ref} as the component of the reflected field.

Again the current expansions of (14) and (15) may be used in the numerical solution for the current distributions. A system of linear equations analogous to (16) is obtained.

Induced Charge Density

Provided the wire diameter is much less than a wave length the induced surface current and charge densities are essentially uniform around the cross section of the wire. In which case the induced surface current density at a given cross section is equal the wire current divided by the wire circumference.

According to the foregoing considerations the induced charge per unit length of the wire is simply related to the wire current. It is[3]

$$Q_1(s_1) = \frac{j}{\omega} \frac{d}{ds_1} I_1(s_1)$$

$$Q_2(s_2) = \frac{j}{\omega} \frac{d}{ds_2} I_2(s_2)$$

in the frequency domain, and in the time domain

$$Q_1(s_1,t) = -\int_0^t \frac{d}{ds_1} [I_1(s_1,t')]dt'$$

$$Q_2(s_2,t) = -\int_0^t \frac{d}{ds_2} [I_2(s_2,t')]dt'$$

where Q_1 and Q_2 are the charge per unit length on wires one and two, respectively.

Pulse Response

To treat pulse response the appropriate Fourier transform of the aforementioned harmonic currents must be performed. This procedure is discussed in a number of Interaction Notes. Obtaining the pulse response requires the evaluation of the following

$$I_1(s_1,t) = \frac{1}{\pi}\int_0^\infty \mathrm{Re}\{I_1(s_1)E_o(\omega)e^{j\omega t}\}d\omega$$

$$I_2(s_2,t) = \frac{1}{\pi}\int_0^\infty \mathrm{Re}\{I_2(s_2)E_o(\omega)e^{j\omega t}\}d\omega$$

where $E_o(\omega)$ is the Fourier transform of the incident pulse.

For convenience a Heaviside pulse is considered incident on the L-wire configuration. If the step variation occurs at $s_1 = s_2 = 0$ and $t = 0$ then

$$E_o(\omega) = \frac{E_o}{j\omega}$$

where E_o is the amplitude of the step in V/m and represents the sum of the incident plus the reflected field, the amplitude of the total electric field.

NUMERICAL RESULTS

In considering an L-Wire configuration over the ground as shown in figure 2 a convenient choice of incident polarization and direction of incidence is made. The direction of incidence is considered to be perpendicular to the plane of the L-wire, and the electric field of the pulse is considered to be linearly polarized vertical to the ground.

At low frequency the current induced on the vertical segment of the L-wire is larger. Furthermore the current distribution induced on the horizontal segment is almost linear. This is shown in figure 3. Also note that numerical instabilities in the solution for the current distribution are occurring in the vicinity of one of the wire ends and the bend of the L. For the data that are presented parameters were chosen to match as closely as possible a parked B-52 (considering only the fuselage and vertical stabilizer or tail structure). Therefore, some of the thin wire assumptions used in deriving (1) are violated. For thin wires the aforementioned numerical instabilities disappear.

As the frequency increases the current along the horizontal section becomes larger than the current along the vertical section which is excited by the incident field. It is soon after this point in frequency that the overall structure resonates. The current distribution on the L-wire is shown in figure 3 for several frequencies. The current distribution presented for the lowest frequency corresponds to the current distribution at the first resonance (see figure 4) of the structure, $k(\ell_f + \ell_t) = 3.2$. If the L-wire were straight this first resonance would occur at $k(\ell_f + \ell_t) \simeq 2.7$ (see Ref. 4). Apparently

a slight tuning effect is occurring. As the frequency is increased it is seen from figure 4 that a second resonance occurs at $k(\ell_f + \ell_t) = 6.3$. Again if the wire were straight this resonance should occur when $k(\ell_f + \ell_t) \simeq 5.6$. The third resonance occurs when $k(\ell_f + \ell_t) = 9.3$. Also near this frequency the tail structure resonates with the fuselage acting as a partial ground plane. If the tail structure were connected directly to a ground plane it would resonate at $k(\ell_f + \ell_t) \simeq 8.1$.

Very sharp peaks in the frequency response occur at the first two total structure resonances. However, the third peak is somewhat wider probably due to a double resonance--a tail structure resonance and a total structure resonance. The relative importance of the peaks depends upon the position along the L-wire where the current is being considered. For example, on the tail structure the third total structure resonance and 1st tail structure resonance are the most significant. But on the fuselage the second and third structure resonances are the most significant. These observations are confirmed in figure 5 where the time histories of the currents are presented for a unit step electric field pulse incident on the structure.

In figure 6 the time history of the induced charge per unit length is shown for a unit step electric field pulse incident on the structure. Note that the induced charge distribution does not approach zero as $t \to \infty$. This occurs because the incident field approaches a static field as $t \to \infty$.

Figure 7 illustrates the pulse (normalized to 1V/m peak) radiated by the vertical dipole facility of the Air Force weapons Laboratory. This pulse is also considered incident on the L-wire configuration. For the model of the B-52 a slightly different set of parameters are used (It is very difficult to arrive at a unique set of parameters for the L-wire to

represent a complex structure such as an aircraft). The frequency response for this new set of parameters is shown in figure 8. Again the general observations made about figure 4 are confirmed.

The time history of the L-wire current induced by the vertical dipole pulse is shown in figure 9. As expected the results are quite similar to those in figure 5. The corresponding induced charge distribution is shown in figure 10. But here the charge distribution differs from the corresponding result in figure 6. This difference occurs primarily because of the considerably different incident pulses for the two cases, and the different physical parameters.

The results presented in figures 8-10 are probably more accurate than the corresponding results presented in figures 3-6 because more current points are used in the former case. Apparently the effect of the ground plane is secondary for both cases.

REFERENCES

1. C. D. Taylor, "Electromagnetic Scattering from Arbitrary Configurations of Wires," Interaction Note 42, November 1968.

2. E. A. Aronson and C. D. Taylor, "Matrix Methods for Solving Antenna Problems," IEEE Trans. Ant. Prop., AP-15, pp. 696-697, September 1967.

3. R. W. P. King and C. W. Harrison, Jr., "Currents, Charges, and Near Fields of Cylindrical Receiving and Scattering Antennas," IEEE Trans. Ant. Prop., Vol. AP-13, No. 6, pp. 978-979, November 1965.

4. F. M. Tesche, "On the Singularity Expansion Method as Applied to Electromagnetic Scattering from Thin-Wires," EMP Interaction Note 102. April 1972.

5. D. R. Wilton, private communication.

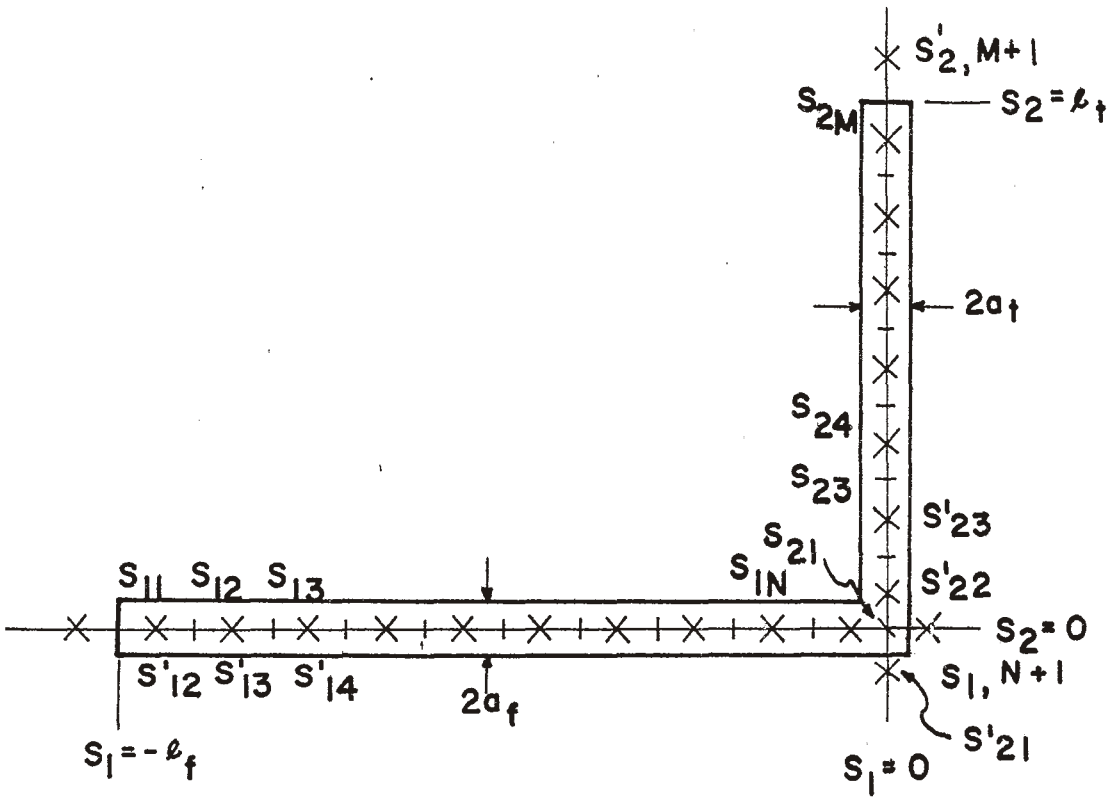

Figure 1: L-Shaped Wire with Current Points.

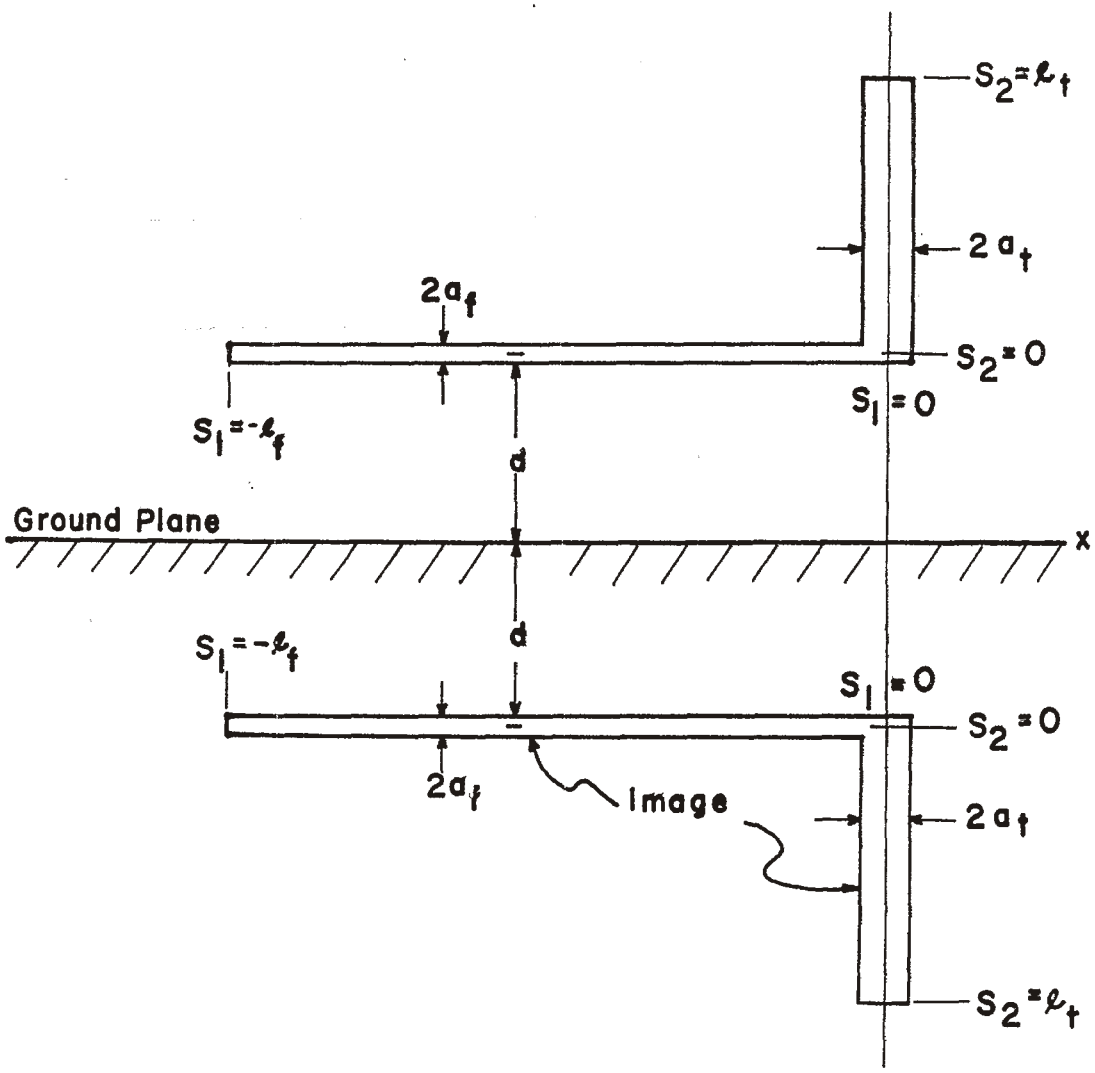

Figure 2: L-Shaped Wire Over a Ground Plane and with Image

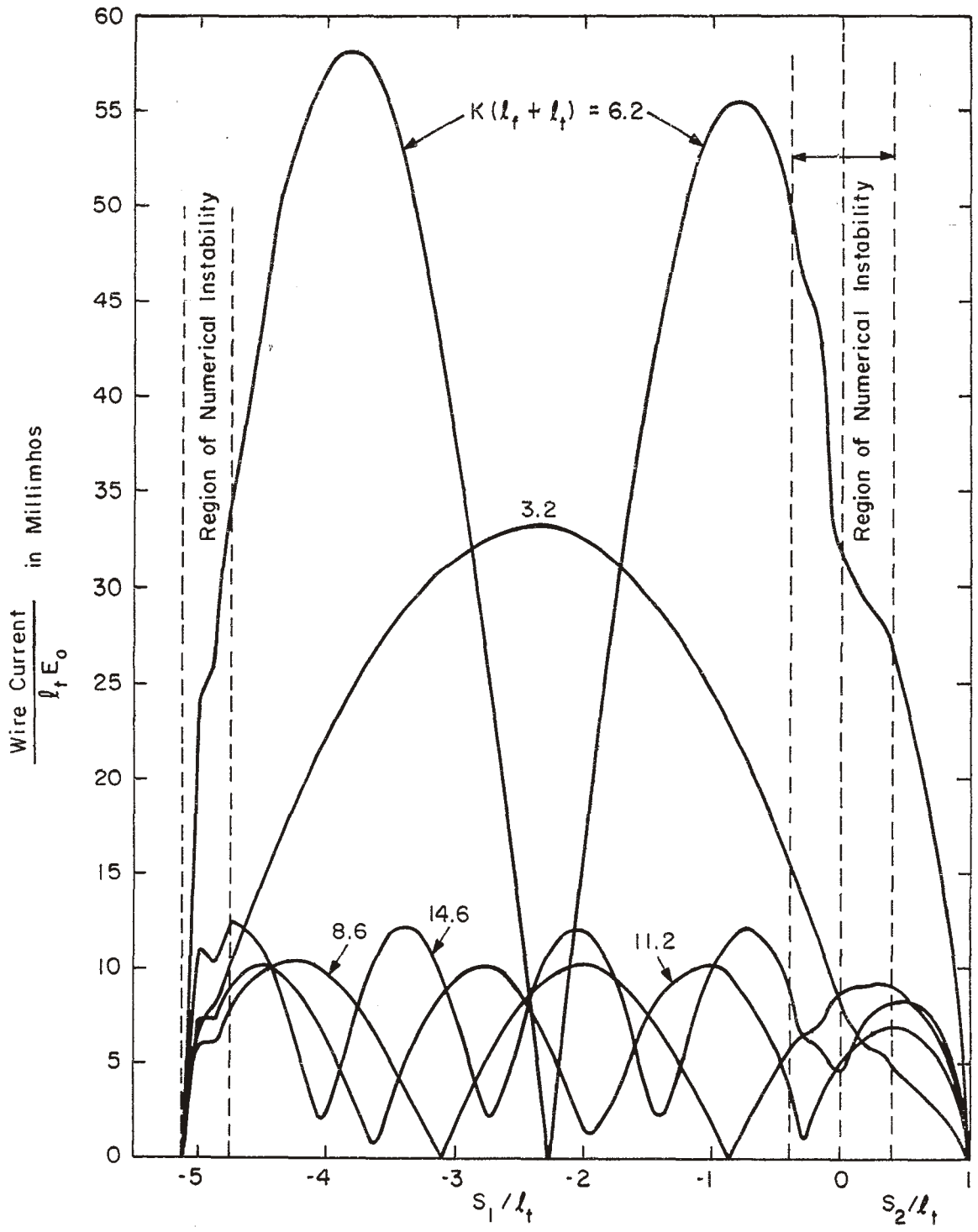

Figure 3: L-Wire Current Distribution for Various Frequencies. $\ell_f/\ell_t = 5.133$, $a_t/\ell_t = 0.0781$, $a_f/\ell_f = 0.0279$, $d/\ell_t = 0.375$, $N = 39$, $M = 7$.

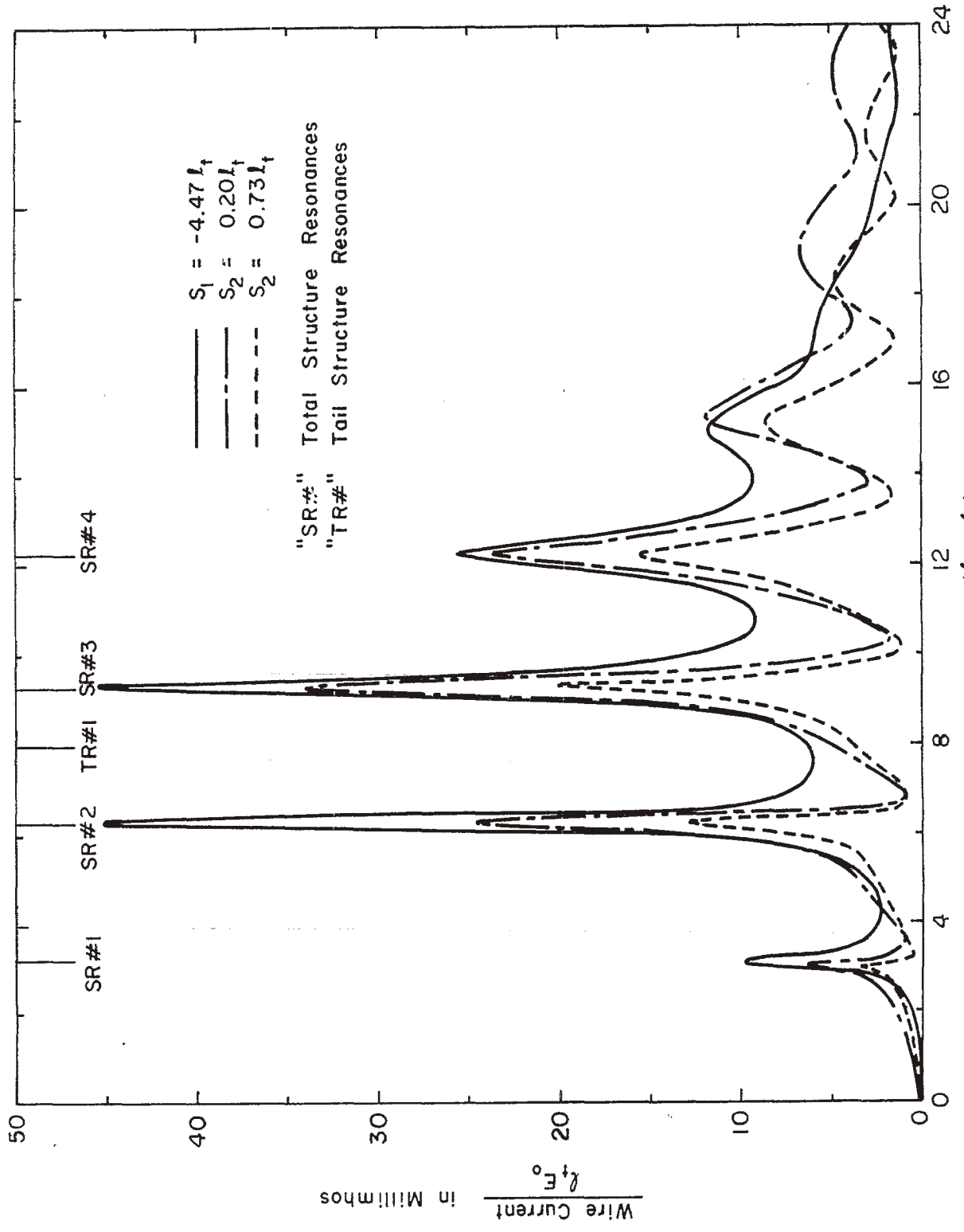

Figure 4. Frequency Response of the Current at Three Points on the L-Wire. $\ell_f/\ell_t = 5.133$, $a_t/\ell_t = 0.0781$, $a_f/\ell_f = 0.0279$, $d/\ell_t = 0.375$, N = 39, M = 7

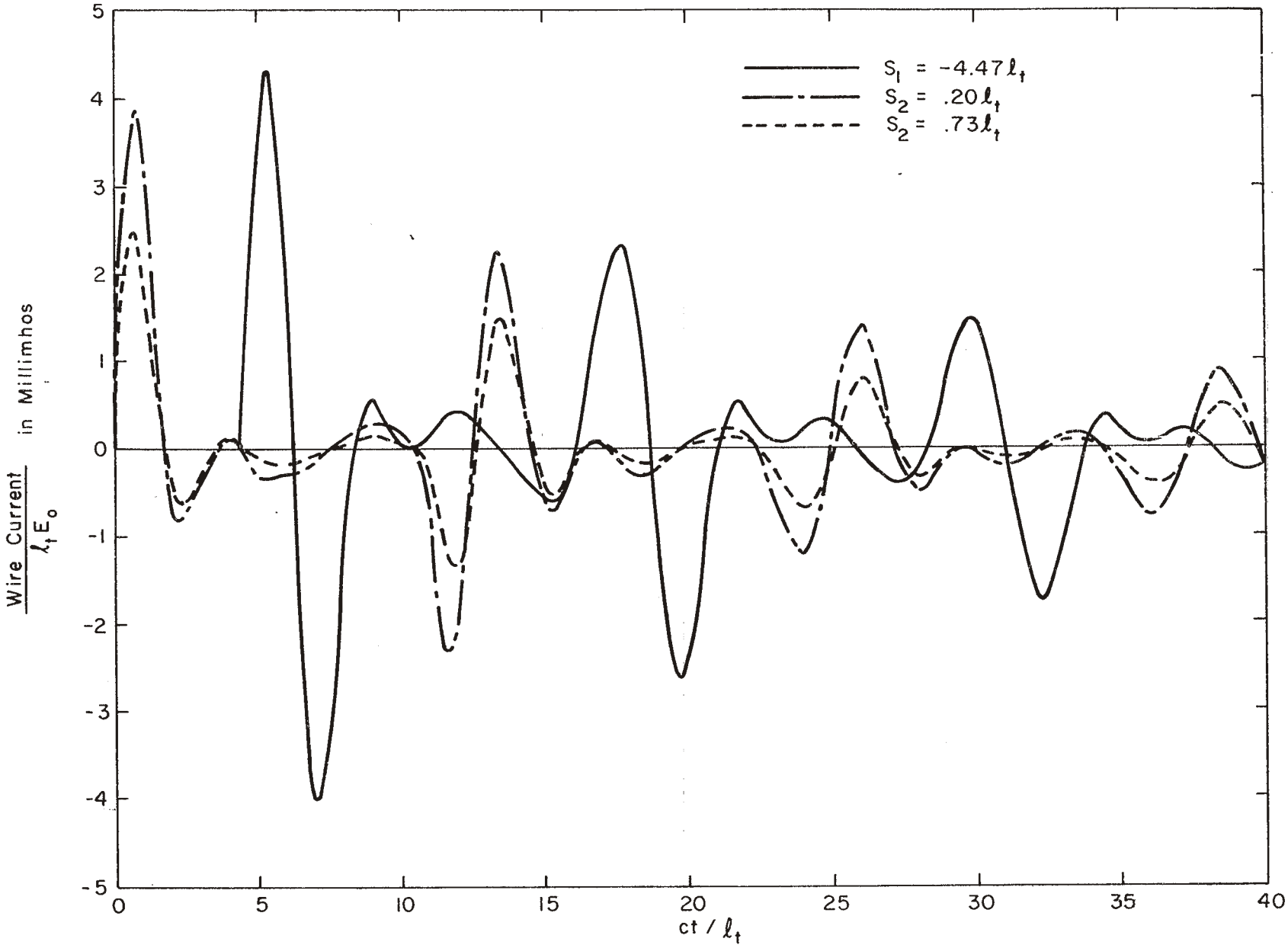

Figure 5. Time History of the Current for Unit Step Incident Pulse. $\ell_f/\ell_t = 5.133$, $a_t/\ell_t = 0.0781$, $a_t/\ell_t = 0.0279$, $d/\ell_t = 0.375$, $N = 39$, $M = 7$

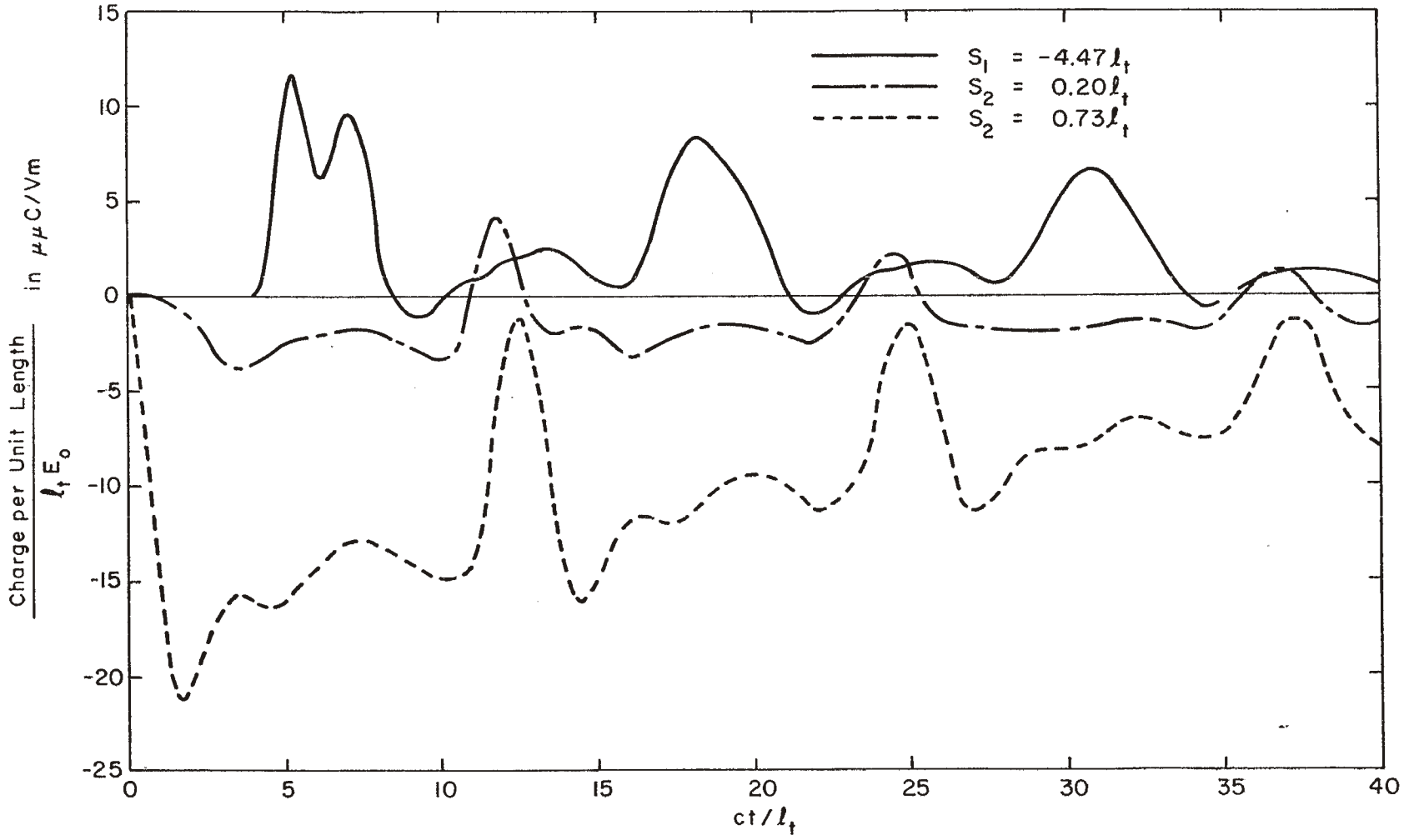

Figure 6. Time History of the Charge Distribution for Unit Step Incident Pulse. $\ell_f/\ell_t = 5.133$, $a_t/\ell_t = 0.0781$, $a_f/\ell_f = 0.0279$, $d/\ell_t = 0.375$, N = 39, M = 7

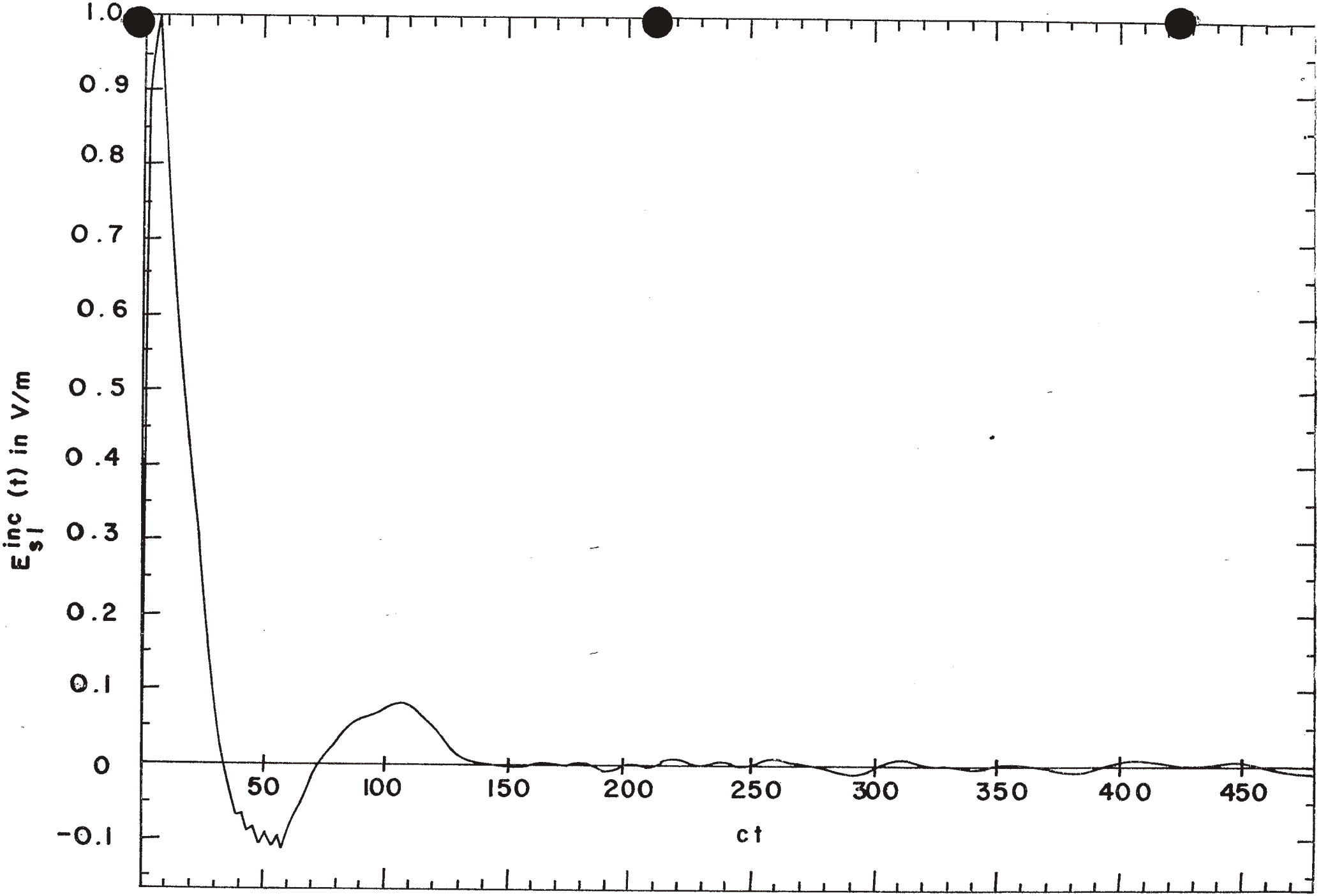

Figure 7: The Time History of the Pulse Considered Incident on the L-Wire.

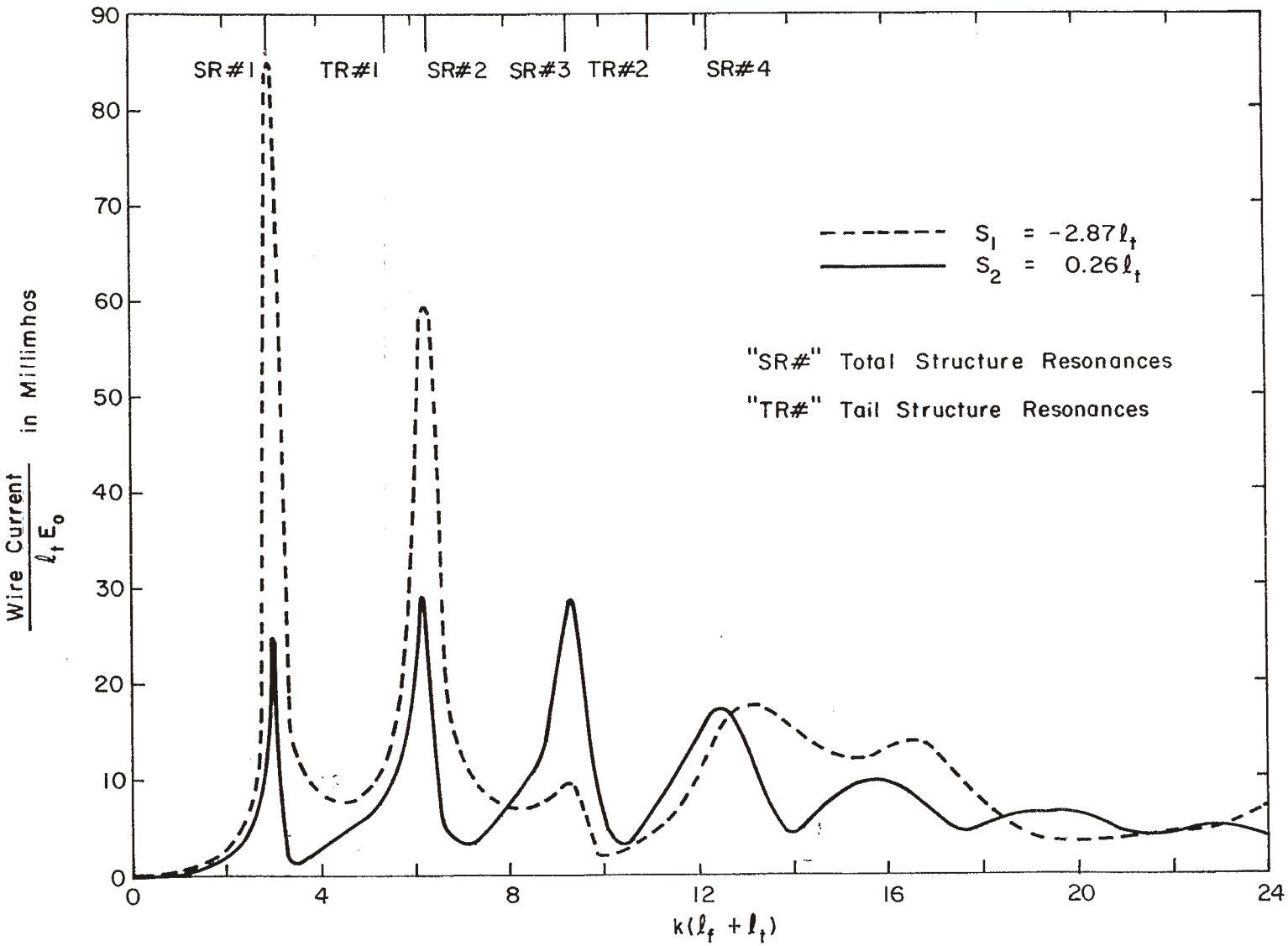

Figure 8: Frequency Response of the Current at Two Points on the L-Wire.
$\ell_f/\ell_t = 4.36$, $a_t/\ell_t = 0.177$, $a_f/\ell_f = 0.044$, $d/\ell_t = 0.293$, $M = 56$, $N = 12$.

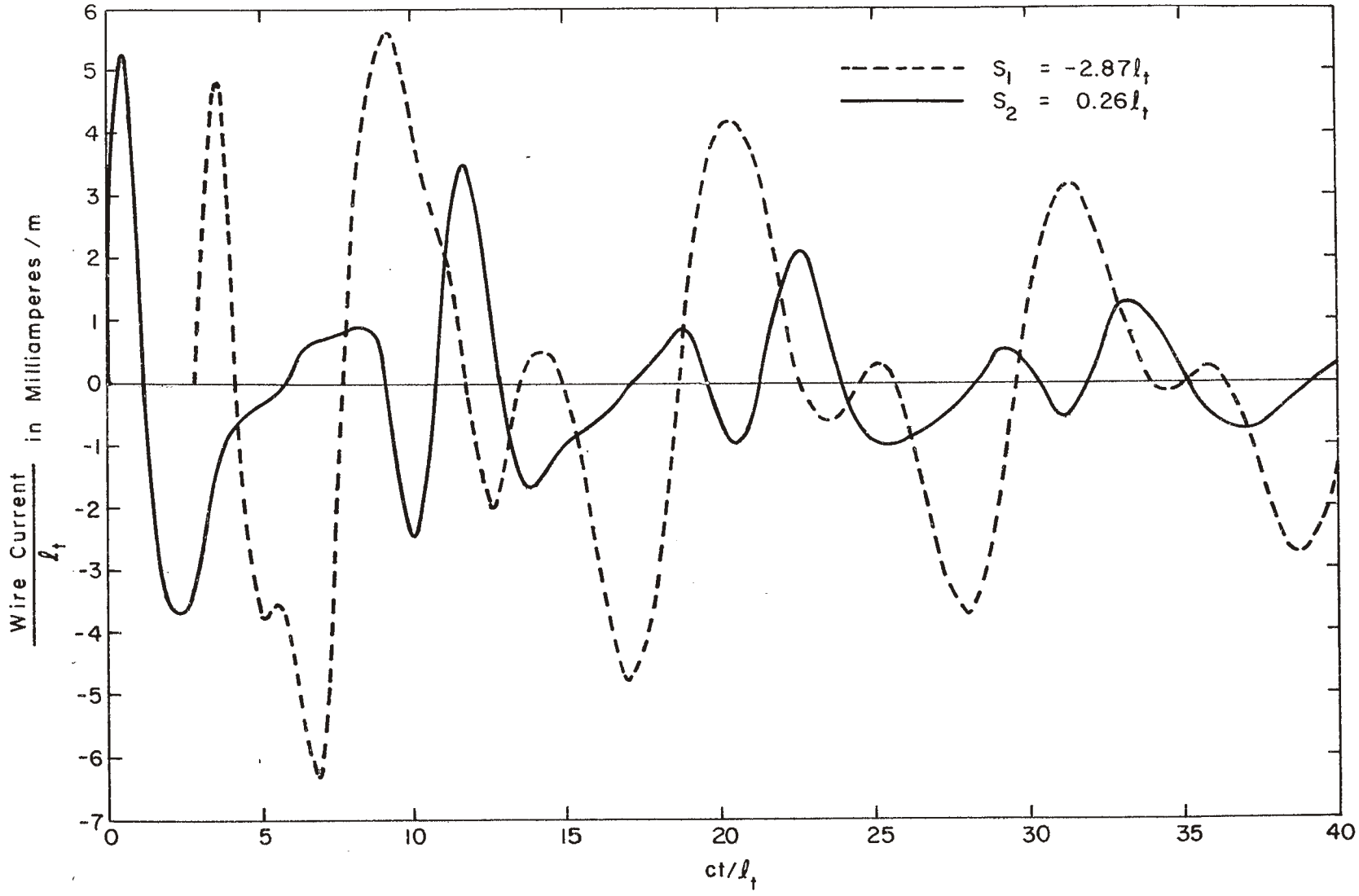

Figure 9: Time History of the Current for the Incident Pulse Given in Figure 7. $\ell_f/\ell_t = 4.36$, $a_t/\ell_t = 0.177$, $a_f/\ell_f = 0.044$, $d/\ell_t = 0.293$, $M = 56$, $N = 12$.

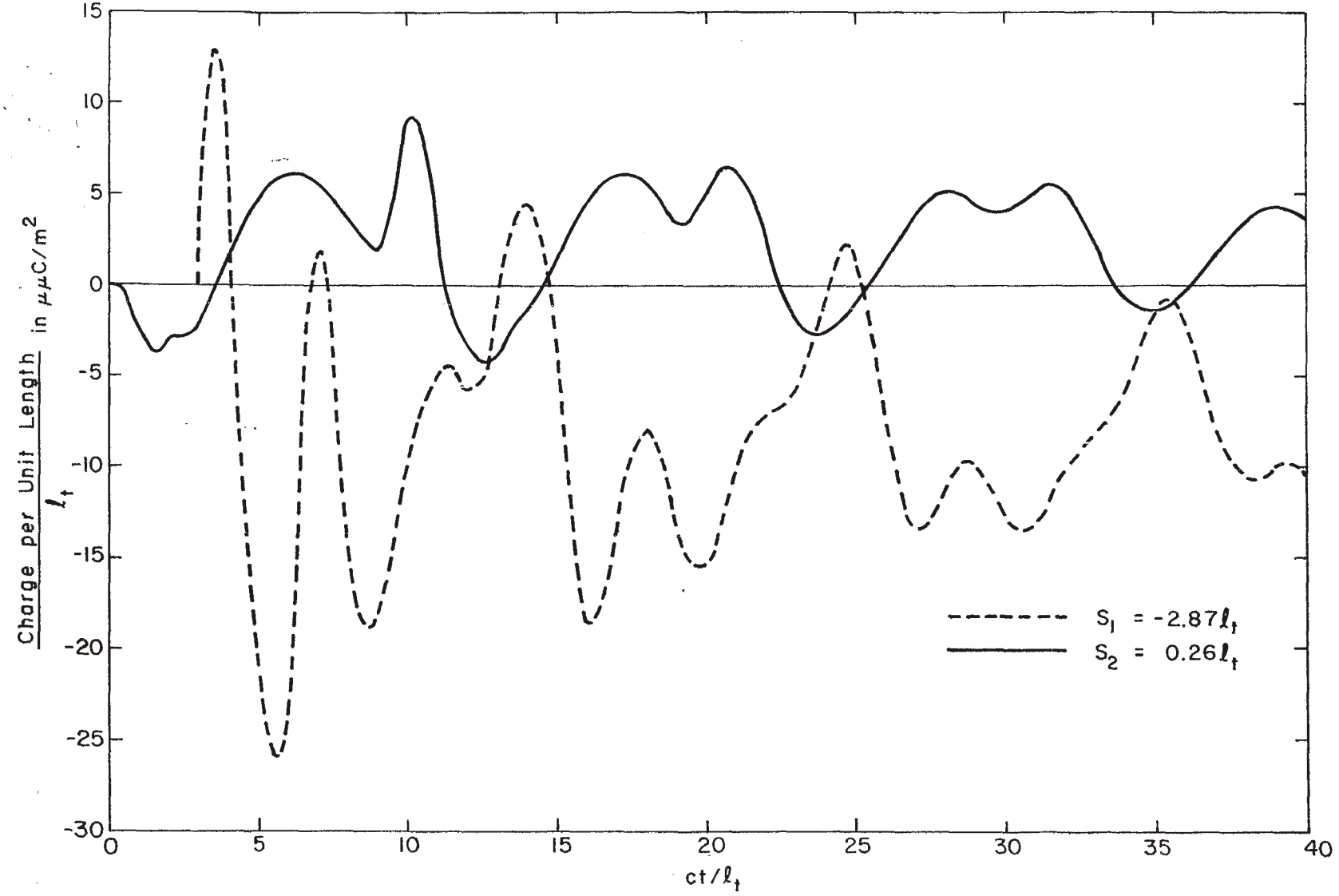

Figure 10: Time History of the Charge Distribution for the Incident Pulse Given in Figure 7. $\ell_f/\ell_t = 4.36$, $a_t/\ell_t = 0.177$, $a_f/\ell_f = 0.044$, $d/\ell_t = 0.293$, $M = 56$, $N = 12$.